DOI: ADD DOINUMBER HERE

Trade-off analysis of a new liquid rocket engine

Filippo Maggi [*], *Davide Zuin* [†], *Simone La Luna* [‡], *Mattia Dotti* [§], *Christian Paravan* [¶], *Luciano Galfetti* [‖]
Politecnico di Milano Dept. Aerospace Science and Technology, 34, Via La Masa, Milano, Italy

Abstract

When high specific impulse and storability are mission requirements, toxic bi-propellant storable couples are very often used. Typically hydrazine or one of its derivatives are used as fuels and nitrogen tetroxide as oxidizer. Maturity of bi-propellant non-toxic alternatives is still low, even though some mono-propellant solutions are coming to the market. The present paper deals with a trade-off for a non-toxic bi-propellant liquid rocket engine based on propene and nitrous oxide, capable of 22 N thrust. The paper explores three different potential architectures and shows some thermal issues arising in the preliminary design of the combustion chamber.

1. Introduction

The search for affordable propulsive solutions with interesting performance levels, featuring low environmental impact, is gaining more and more importance. These propellants are generally easier to handle, they involve lower level of safety requirements and, lower recurrent costs. This scenario is considered a viable method to bring down the costs associated with propellant transport and storage, and with spacecraft development and on-ground operations. At the same time, the maturity level of the non-toxic propellant family has grown fast in the last decade. The mono-propellant group was the most developed one, showing strong achievements, for example in the field of the ionic compounds. As an example we should consider the liquid ADN (ammonium dinitramide) liquid solution which results in non-toxic, non-explosive, high-performance replacement of hydrazine. Current applications are demonstrating the substantial maturity of the basic technology and the readiness for space flights.[1] On the side of the bi-propellants, the development is still lacking strong momentum.

A storable bi-propellant is a complex solution requiring a redox reaction after spraying, vaporization, and mixing. The addition of a catalyst may help the reaction of one of the compounds. With respect to cryogenic or semi-cryogenic solutions, a lower level of specific impulse is obtained. At the same time, storability grants longer mission possibility and lower thermal management requirements once in orbit. Application to moderate ΔV and thrust missions, such as orbit change, makes bi-propellant still attractive with respect to mono-propellants. The superior specific impulse reduces the propellant load even though the inert mass is higher. Typically, pressure-fed architecture is preferred for simplicity and dry weight considerations, using either blow-down or regulated pressurizing condition.

Long-term storage capability is an appealing solutions for military applications or low-thrust space rocket engines. These chemicals are easily found in large first and second stages of ballistic missiles because they allow almost instantaneous readiness without the delays and precautions that come with cryogenic propellants. The hypergolic nature of most of these combinations is exploited in space missions, granting multiple reignitions using reliable and simple architecture (namely, no ignition device is required). Toxicity is often an issue. The main couple used so far in space-related devices is represented by nitrogen tetroxide and a hydrazine derivative. It is interesting to note that, whereas multiple liquid storable fuel solutions exist even with virtual zero-level toxicity, the scenario for liquid oxidizers is quite limited if the choice is restricted to chemicals readily available in large scale. In a paper by Edwards published in 2003 a list of storable propellants is discussed.[2] Eight liquids are mentioned. In this group only three were oxidizers and only one is currently considered a green one.

The selection of a propellant couple follows a set of general criteria. An initial and non-exhaustive list of selection guidelines is reported here:

[*] filippo.maggi@polimi.it, Associate Professor, Space Propulsion Laboratory, corresponding author
[†] davide.zuin@mail.polimi.it, M.Sc. Student
[‡] simone.laluna@mail.polimi.it, M.Sc. Student
[§] mattia.dotti@mail.polimi.it, M.Sc. Student
[¶] christian.paravan@polimi.it, Adjunct Professor, Space Propulsion Laboratory
[‖] luciano.galfetti@polimi.it, Full Professor, Space Propulsion Laboratory

- economic factors (e.g. adequate supply chain with reasonable cost);
- propulsion performance (combination of high energy content and low molecular mass of the product gases);
- material compatibility (e.g. avoiding risk of self-decomposition);
- health hazards (e.g. for operators as well as for accident scenarios);
- corrosion of containers and pipes (partially connected to compatibility);
- stability (e.g. limited or no decomposition under a wide range of conditions and time);
- ignition and flame properties (e.g. hypergolic nature);
- high specific gravity (promoting high energy-density storage);
- vapor pressure (e.g. promoting either vaporization or self-pressurization);
- cooling methodology (e.g. thermal properties for regenerative cooling, if needed).

Everybody is aware that the replacement of toxic compounds is not a cheap solution. The TRL advancement requires investments and time. Most of the propellant properties listed above are in some manner interacting with the general cost of a propulsion system, throughout its whole life cycle, from the development to use and disposal. In this respect, the analysis in a paper by Schmidt and Wucherer has touched some of these aspects drafting a cost/benefit analysis on a more comprehensive perspective.[3] The authors claim that their attempt is the first one looking at the economic question on a general perspective. In any case, the scenario is probably more complex and requires more general analyses to obtain a reliable perspective.

2. The propulsion system

2.1 Main assumptions

The present paper aims at analyzing a hypothetical bi-propellant pressure-fed rocket motor which uses the storable couple N_2O/C_2H_6. Nitrous oxide (N_2O, enthalpy of formation $\Delta H_f = 82.05\,\mathrm{kJ\,mol^{-1}}$) is a non-toxic, stable and storable oxidizer. It is a non-corrosive liquid and can be used with common structural materials. It features a vapor pressure higher than the atmospheric one, so its storage requires pressurized vessel containment. The vapor pressure is strongly dependent on temperature. Its critical temperature is at 309 K while the critical pressure is at 72.51 bar.[4] The proximity to the critical point makes the density quite low. For example at the temperature of 298 K the density is $743.9\,\mathrm{kg\,m^{-3}}$ and the vapor pressure is 56.74 bar. The thermal decomposition can be observed from about 600 °C. Propene (C_3H_6, enthalpy of formation of the gas phase under standard conditions $\Delta H_f = 20.41\,\mathrm{kJ\,mol^{-1}}$) is a colorless, non-toxic, nor carcinogenic gas *. Similarly to nitrous oxide, also propene is characterized by high vapor pressure. Its boiling point at ambient temperature is 225.46 K. Liquid storage is possible under pressurized conditions. Its critical temperature is at 364.9 K while the critical pressure is at 46.00 bar. The vapor pressure at ambient temperature (298 K) is 11.53 bar

A 22 N single-burn rocket motor discharging in vacuum is considered. Propellant mass budget is computed for three different possible missions having the total impulse of 30 kN s, 110 kN s and 220 kN s. Expansion ratio $\varepsilon = 200$ was chosen, with a divergent nozzle based on Rao approximation with 80 % length of the corresponding conical reference nozzle (semi-angle of 15°).[5] On the basis of similar compositions and without specific data, the characteristic length of the chamber is assumed $L^\star = 1$ m and the contraction ratio is 10. The combustion chamber P_c is initially assumed to operate in the pressure range between 3 and 30 bar, then limited to a maximum of 10 bar for technological issues. The resulting internal combustion chamber radius spans from 6.14 mm for $P_c = 10$ bar up to 11.2 mm for $P_c = 3$ bar. When needed the environmental temperature is fixed at the standard condition $T_{env} = 298.15$ K.

Tanks containing the propellant are cylinders or spheres depending on specific configuration. An ideal (volume-less and mass-less) inner diaphragm seals the section and separates liquid and vapor fractions. Construction material of the pressure-tight part is carbon fiber. Burst pressure margin is 2. The vessels are equipped with a sharp-edged drilled hole having discharge coefficient $C_d = 0.65$. Independently from the configurations of tanks and propellant state (liquid or gaseous), fluid properties inside each vessel are considered isotropic and their propagation is instantaneous.

*World Health Organization, International Agency for Research on Cancer, last consulted, 26/06/2019

2.2 Propellant discharge

The use of self-pressurizing propellants stored in liquid phase makes the modeling of their discharge complex. Often the flow conditions make the liquid operate across the saturation line in the pipes or in the injectors. Nitrous oxide description, based onto ideal gas and compressible or incompressible flow assumption, cannot be applied due to its compressibility factor Z, which in saturation conditions differs significantly from the ideal case. Dyer and co-authors report for the vapor $Z_v = 0.13$ while for the liquid phase $Z_l = 0.53$, making the assumptions of both incompressible liquid and perfect gas inadequate.[6] The same authors presented the NHNE (non-homogeneous non-equilibrium) engineering model, further corrected by Solomon[†] in his M.Sc. thesis.[7] The model blends the typical incompressible model of a fluid discharging across an orifice with the Homogeneous Equilibrium Model (HEM) on the basis of a weighting parameter W and a non-equilibrium parameter k, reported in Eq. 1 and 2.

$$W = \frac{1}{1+k} \tag{1}$$

$$k = \sqrt{\frac{p_{tank} - p_{out}}{p_{vap} - p_{out}}} \tag{2}$$

The upstream fluid vapor pressure P_{vap} is defined as the total pressure for a saturated fluid, the total pressure in the tank is P_{tank} and P_{out} is the static pressure outside the vessel. Under the assumption of isenthalpic flow, the NHNE model equation becomes the formula reported in Eq. 3. The computation grounds on the mass flow rate obtained from the incompressible formula $\dot{m}_{inc} = C_d A \sqrt{2\rho\Delta p}$, where A is the orifice cross section, ρ is the fluid density, and Δp is the pressure drop across the orifice.

$$\dot{m} = (1 - W)\,\dot{m}_{inc} \tag{3}$$

The same approach has been applied for the modeling procedure of the self-pressurized propene discharge. It should be noted that the propellant couple can perform partial or total self-pressurization. Nitrogen pressurizing agent is adopted when the former option is not feasible due to constraints imposed by the combustion chamber pressure.

Typical pressure loss values have been obtained from the literature.[8,9] Concentrated losses are assumed for orifices and injection plate. Losses in pipes are discarded at this stage

2.3 Configuration for propellant mass trade-off

The propellant mass trade-off analysis explored three possible tank configurations and the combustion pressures of 3 bar and 10 bar. Time-discretized discharge procedures have been implemented, constraining the total impulse requirement. The code implements a minimum search for the wet mass of the system where orifices and propellant amount are varied to obtain the firing time imposed by the total impulse constraint. The dump from the tank to the feeding line is performed under isenthalpic conditions implementing an iterative computation for pressure matching.

Case A This is the main case of interest, involving self-pressurization of both oxidizer and fuel using their own vapor pressure (Fig. 1a). This case is interesting since self-pressurization avoids the implementation of additional pressurization systems, which increase the mass budget of the propulsion subsystem. This option cannot be used for the 10 bar case because the self-pressurization capability of propene is not high enough.

Case B This architecture exploits the self-pressurization capability of the oxidizer and use it to operate the fuel tank. The direct contact is avoided using a small buffer tank containing nitrogen (Fig. 1b). The interface diaphragms have been modeled as ideal piston capable of moving without friction inside the nitrogen tank. This case presents no heritage and involves complex design of the tank and feeding systems. The addition of a N_2 tank increases the mass allocated to the propulsion system and the solution algorithm complexity. Two discharge procedures are considered from the same oxidizer tank. Vapor valve lets only gaseous N_2O out for nitrogen pressurization while the liquid phase exits from the main valve to the combustion chamber.

Case C The option considers in parallel a self-pressurized oxidizer and a fuel pressure-fed system with N_2 as pressurizer fluid at the same initial pressure of the oxidizer. Phase separation is granted by ideal diaphragms (Fig. 1c). In this case, the system is characterized by the highest heritage derived from the flight history of resistojet thrusters with self-pressurized N_2O tanks[10] and blowdown systems.[8]

[†]The reader should be aware that a typo error is probably present in the original document by Solomon in Eq. 2.18 and 2.21, as the area A_c should not be present.

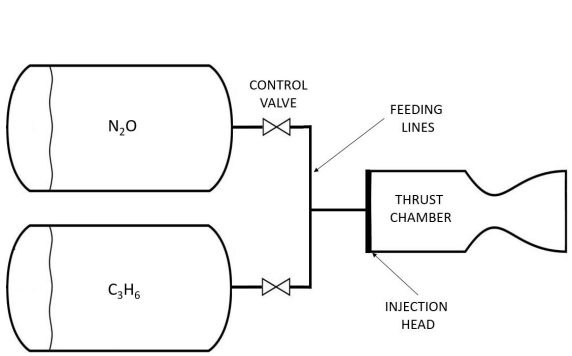

(a) Case A

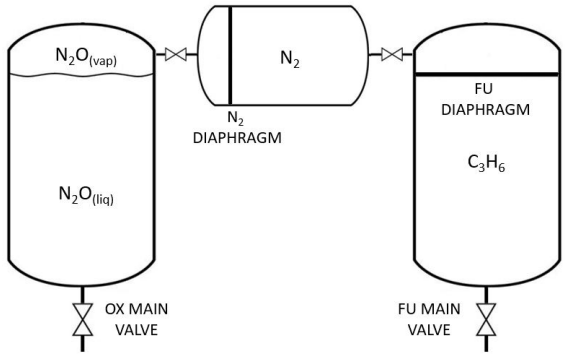

(b) Case B

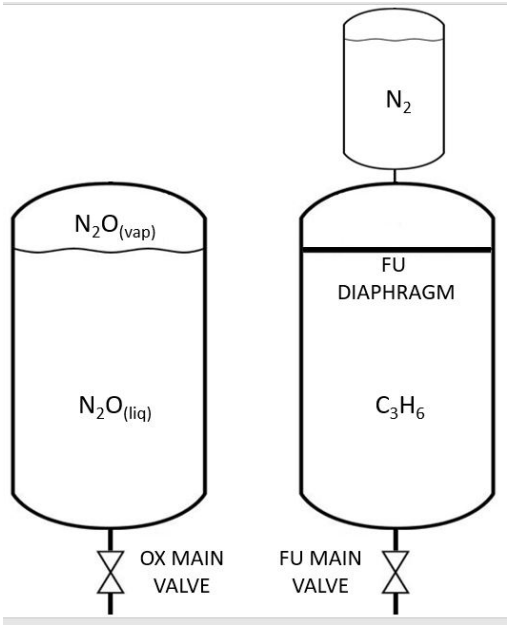

(c) Case C

Figure 1: Tank configurations explored for mass-volume trade-off analysis

2.4 Configuration for thermal trade-off

The preliminary thermal analysis was performed using the RPA (Rocket Propulsion Analysis) code on the basis of the Bartz method.[11] Regenerative cooling only is considered, using nitrous oxide after complete phase transition from liquid to vapor. All the mass flow rate of N_2O has been considered for the cooling, injected in counter-flow direction to maximize the heat transfer. Inclination of the channels were assumed from 0° to 60° with respect to the axis of the motor. The geometry of the channel is reported in Fig. 2, assuming $b = 1$ mm, $h_c = 1.5$ mm and $h = 1$ mm. The size of a changes along the rocket length and has a maximum of 5.4 mm at the head end of the combustion chamber and a minimum in the throat of 1.6 mm. Nitrous oxide is injected from just downstream this point. The last part of the nozzle (divergent part) is radiatively cooled, using the same thickness and material (Inconel 718). Cases up to 10 bar were analyzed. Higher pressure cases were rejected for thermal issues.

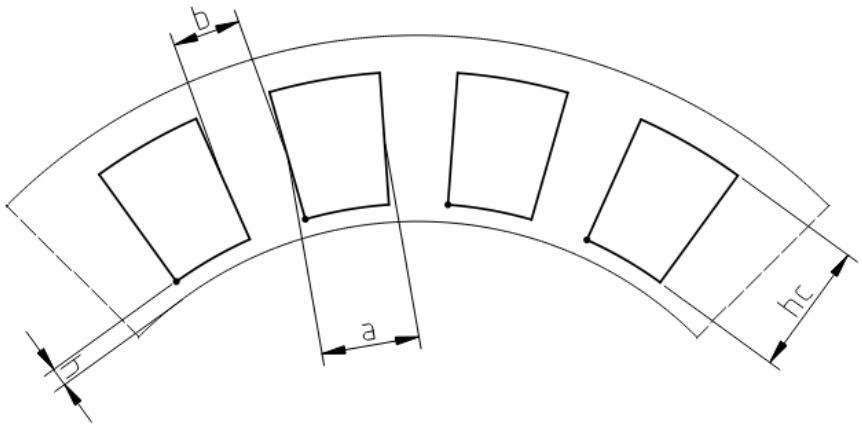

Figure 2: Cooling jacket geometry

Thermal conductivity and viscosity variation with temperature of the coolant fluid have been recovered from the literature. Viscosity of liquid phase in the temperature range between 220 K and vaporization were retrieved from the literature. A conference paper by Zimmerman and co-authors observes that some thermophysical properties of nitrous oxide and carbon dioxide differ of few percent.[12] That is, the liquid viscosity is approximated with the one of the CO_2, as dedicated data are not available. Viscosity values for gas phase are originated from.[13] Thermal Conductivity for liquid nitrous oxide is derived from the saturated conditions of the NIST webbook [‡] and for gas phase from.[14]

3. Results

The vacuum specific impulse of N_2O/C_3H_6 couple for the case relevant to the present paper is reported in Fig. 3. The value assumes 95 % efficiency and 2D losses. The combustion chamber pressure spans in the range 3 bar to 30 bar. The adiabatic flame temperature is reported in Fig. 4. The oxidizer-to-fuel ratio for highest specific impulse is between 6.5 to 7.0 with a decrementing trend as the combustion pressue is incremented. The maximum temperature is located at a bout 7.7, with minor influence from the chamber pressure. Both curves do not have a narrow peak. For the specific impulse, only 1 % decrement is obtained when the oxidizer-to-fuel ratio is changed of one unit around the maximum. Same considerations can be done on the flame temperature.

[‡]http://webbook.nist.gov

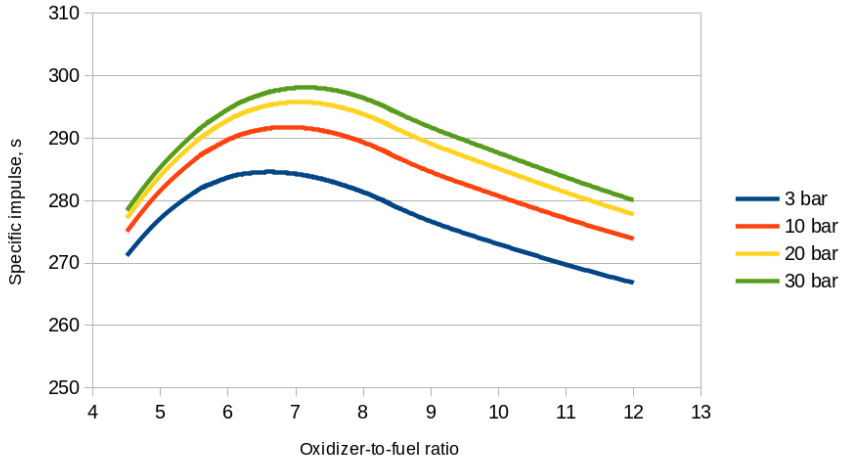

Figure 3: Vacuum specific impulse of N_2O/C_3H_6, expansion ratio 200, 95 % efficiency, 2D losses.

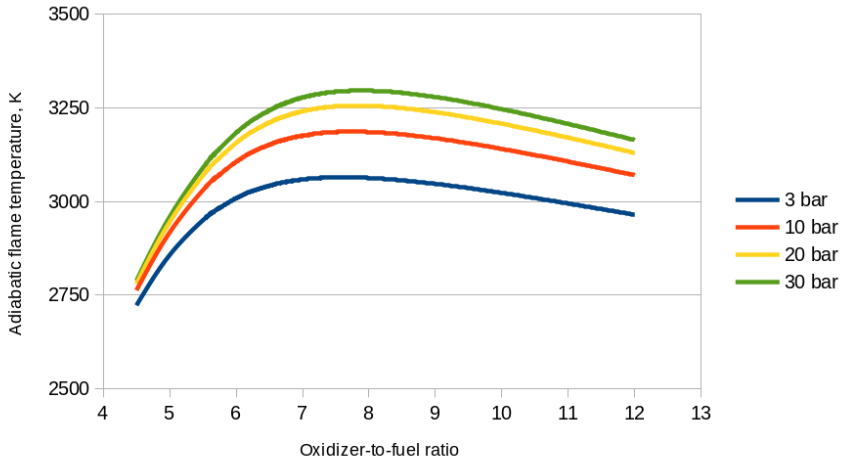

Figure 4: Adiabatic flame temperature of N_2O/C_3H_6

3.1 Peculiarity of self-pressurization tanks

In Case A the tanks are self-pressurized. This use causes an evident non-constant flow behavior during the propellant expulsion. As reported in Fig. 5, the temperature decrements progressively during firing (Fig. 6). The liquid fraction evaporates to fill up the empty space left by the propellant. Both liquids feature peculiar thermodynamic and physical properties which translate into different temperature and pressure histories in the tanks as well as non-uniform losses along the pipelines. As a consequence, oxidizer-to-fuel shift is observed, producing an alteration of the specific impulse.

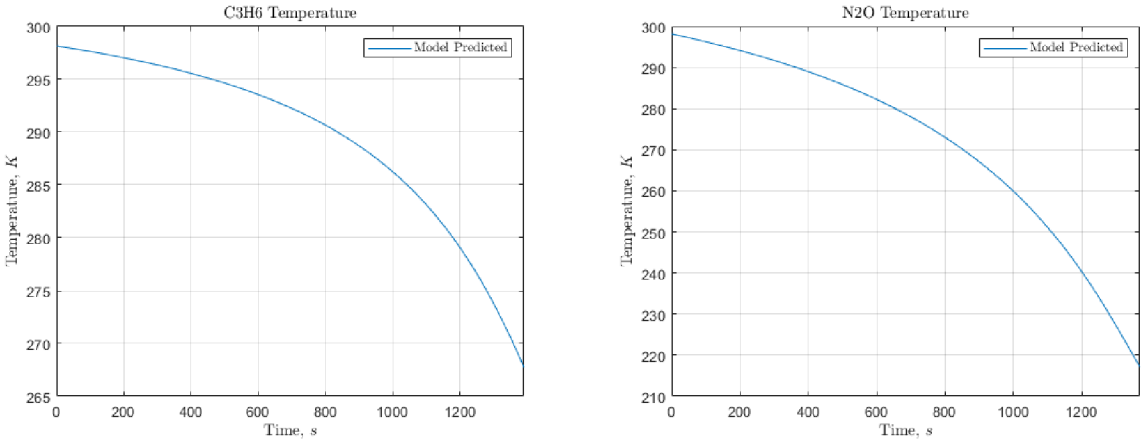

(a) Fuel (b) Oxidizer

Figure 5: Temperature in self-pressurized tanks during firing for case A. $I_{tot} = 30\,\text{kN s}$, $P_c = 3\,\text{bar}$.

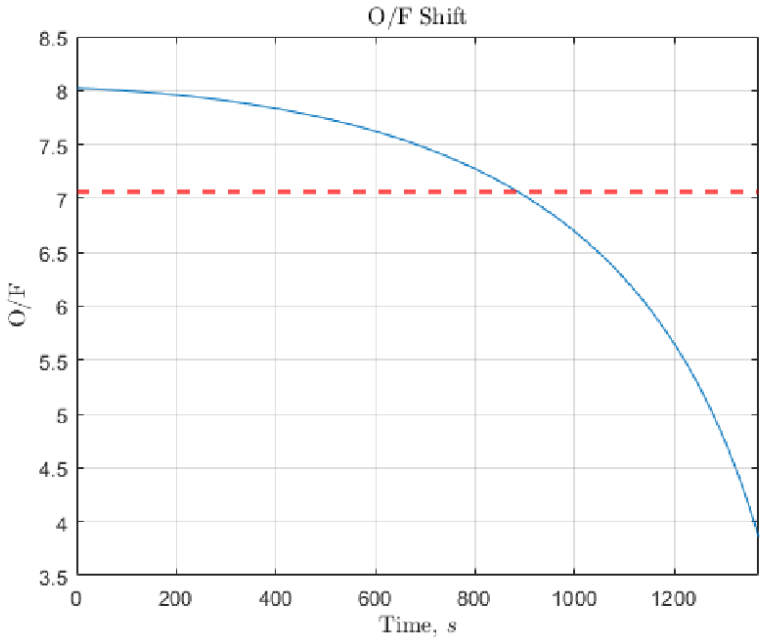

Figure 6: Oxidizer-to-fuel shift during firing for case A. Red dashed line: averaged value.

3.2 Mass budget considerations

For better approximation, the vacuum specific impulse used for mass budget was evaluated through the Bray expansion model with the freezing point in the throat. The effective impulses, including also two-dimensional losses, were

$I_{s-vac}(3\,\text{bar}) = 284.6\,\text{bar}$ and $I_{s-vac}(10\,\text{bar}) = 291.8\,\text{bar}$. The comparison focused on total propellant mass, pressurizing supplements (pressurant tank and nitrogen), and feeding line inerts accounted for 15 % of the propellant mass. Oxidizer and fuel tank weight was not investigated. In Tables 1 and 2 the trade-off was reported respectively for the motor running at the combustion chamber of 3 bar and 10 bar. The configuration exploiting the self pressurization of both

Table 1: Mass budget for $P_c = 3\,\text{bar}$, data in kg

Total impulse, kN s	30	110	220
Conf. A	14.14	48.88	99.24
Conf. B	14.62	49.75	99.43
Conf. C	14.81	49.45	99.40

Table 2: Mass budget for $P_c = 10\,\text{bar}$, data in kg

Total impulse, kN s	30	110	220
Conf. A	N.Av.	N.Av.	N.Av.
Conf. B	14.74	51.32	99.72
Conf. C	15.24	54.10	112.86

reactants (Case A) can be operated only in the low pressure case because of the limited vapor pressure of the propene at the storage condition, further decreased by pressure losses in pipes, valves, and injector head. For the low pressure condition good similarity with respect the three architectures is obtained. Within the same total impulse constraint, the three entries differ only for few hundreds of grams The scenario is rather different in the case with high pressure combustion. The worst scenario is represented by the Case C, where the oxidizer is self-pressurized and a nitrogen tank pressurizes the fuel. The difference is inherited by the dynamics imposed by the architecture. On the one side, more propellant mass is required when it is used also as pressurizing agent. The Case B is characterized by an additional inert mass represented by the piston/bladder combination. Similar inert mass is present in Case C for the fuel tank only. This seems to be the most penalized configuration.

3.3 Thermal analysis

The typical thermal pattern in the rocket motor is reported in Fig. 7. The case corresponds to the rocket motor working at 3 bar with inclination of the cooling channels of 0° with respect to motor main axis. As expected, the highest heat flux is located in the throat and quickly decrements in the divergent part. The coolant, injected in counter-flow at the throat section, increases its temperature while the internal wall temperature follows the trend of the heat flux, with a peak at the throat.

Parametric analysis on pressure and coolant flow inclination are summarized in Fig. 8. By increasing the angle of the cooling jacket direction with respect to the main axial direction, the hot gas wall temperature decrease. At the same time the temperature of the N_2O coolant tends to increase up to the point where dissociation occurs. This creates a problem in the management of the thermal loads. Whereas on the one side the cooling of the wall should verify the Inconel 718 working range (up to about 1000 K), on the other side the nitrous oxide should be maintained below its decomposition temperature. From the bar plots it is clear that such condition cannot be realized. It appears that, in said configuration, the amount of the oxidizer used as cooling flow is not enough. Moreover, N_2O is not characterized by high heat capacity. At ambient temperature the value is $0.88\,\text{J}\,\text{kmol}^{-1}\,\text{K}$, much lower than gaseous hydrogen which features $14.32\,\text{J}\,\text{kmol}^{-1}\,\text{K}$. Propene has a better thermal behavior with a specific heat at constant pressure of $1.5\,\text{J}\,\text{kmol}^{-1}\,\text{K}$ but the amount is much lower than the oxidizer and does not suffice.

4. Final remarks

This trade-off analysis has addressed one of the possible green alternatives for space bi-propellants rockets. Three architectures have been investigated, trying to exploit the self-pressurizing attitude of either oxidizer alone or both reactants. From the propellant mass budget viewpoint, the configurations are quite equivalent when a limited total impulse is requested. Case 3 seems to bring an additional propellant mass budget for higher I_{tot}. Case 1 can be implemented only for low pressure conditions. The thermal analysis gives negative perspectives. Temperature values of the hot mixture in the CC exceed the capabilities of the system to survive the thermal loads. The amount of oxidizer is not enough to remove heat maintaining the fluid below the decomposition point and, although pressure increment

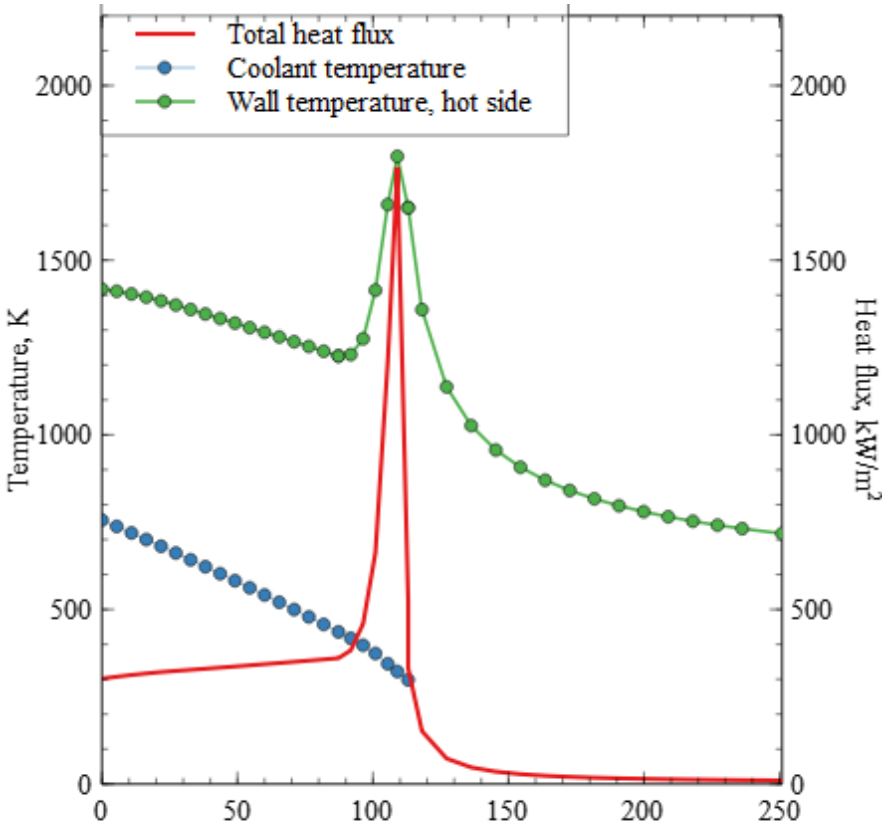

Figure 7: Thermal analysis of rocket motor working at 3 bar with straight cooling channels

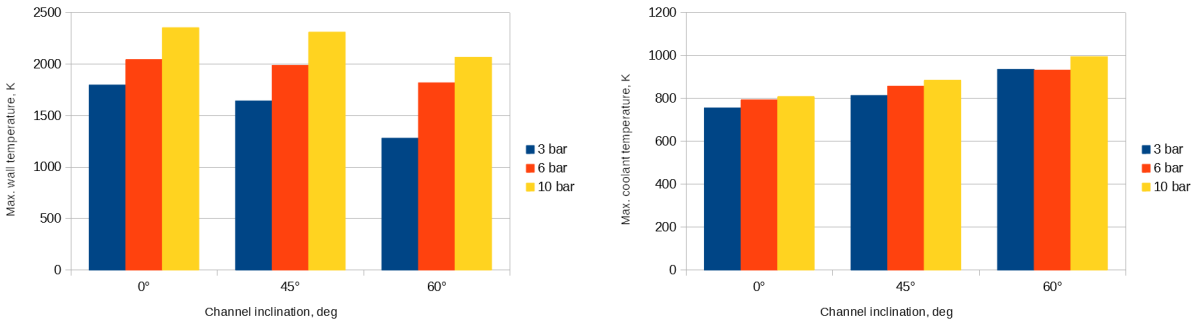

(a) Fuel

(b) Oxidizer

Figure 8: Maximum temperatures for tested cases

improves propulsion performance, worse thermal loads are obtained. Evolutions of this case study are evaluating additional cooling strategies such as high-temperature ceramic coatings and film cooling at the walls. The change of the type of Inconel may also extend the thermal capability.

References

[1] K. Anflo and B. Crowe. In-space demonstration of an ADN-based propulsion system. *AIAA paper*, 2011-5832, 2011.

[2] T. Edwards. Liquid fuels and propellants for aerospace propulsion: 1903-2003. *Journal of Propulsion and Power*, 19(6):1089–1107, nov 2003.

[3] E. W. Schmidt and E. J. Wucherer. Hydrazine (s) vs. nontoxic propellants. where do we stand now? In *Second international conference on green propellants for space applications*, 2004.

[4] AA.VV. Thermophysical properties of nitrous oxide. Technical Report 91022, Engineering Sciences Data Unit (ESDU), 1991.

[5] G. V. R. Rao. Exhaust nozzle contour for optimum thrust. *Journal of Jet Propulsion*, 28(6):377–382, 1958.

[6] J. Dyer, G. Zilliac, A. Sadhwani, A. Karabeyoglu, and B. Cantwell. Modeling feed system flow physics for self-pressurizing propellants. *AIAA paper*, 2007-5702, 2007.

[7] B. J. Solomon. Engineering model to calculate mass flow rate of a two-phase saturated fluid through an injector orifice. mathesis, Utah State University, 2011.

[8] J. P. Sutton and O. Biblarz. *Rocket Propulsion Elements*. Wiley, New York, NY, USA, seventh edition, 2001.

[9] R. W. Humble, Henry G. N., and W. J. Larson. *Space Propulsion Analysis and Design*. McGraw Hill, first revised edition, 1995.

[10] V. A. Zakirov. *Investigation into Nitrous Oxide Propulsion Option for Small Satellite Applications*. phdthesis, Univer ity of Surrey, Surrey, UK, 2001.

[11] A. Ponomarenko. RPA - tool for rocket propulsion analysis. In *Space Propulsion Conference, Cologne, Germany*, 2014.

[12] J. Zimmerman, B. Cantwell, and G. Zilliac. Initial experimental investigations of self-pressurizing propellant dynamics. *AIAA paper*, 2012-4198, 2012.

[13] M. Takahashi, N. Shibasaki-Kitakawa, C. Yokoyama, and S. Takahashi. Viscosity of gaseous nitrous oxide from 298.15 k to 398.15 k at pressures up to 25 MPa. *Journal of Chemical & Engineering Data*, 41(6):1495–1498, 1996.

[14] J. Millat, M. Mustafa, M. Ross, W. A. Wakeham, and M. Zalaf. The thermal conductivity of argon, carbon dioxide and nitrous oxide. *Physica A: Statistical Mechanics and its Applications*, 145(3):461–497, 1987.